Reversal of pathologic changes in fibroblasts from Niemann-Pick type C disease patients by inhibition of bromodomain and extraterminal proteins

Martina Parente[1], Amélie Barthelemy[2], Claudia Tonini[1], Alessandra Sacchi[1], Stefano Leone[1], Marco Segatto[3], Frank W. Pfrieger[2*], Valentina Pallottini[1,4*]

[1]Department of Science, Section Biomedical Science and Technology, University Roma Tre, Viale Marconi 446, 00146 Rome, Italy.

[2]Centre National de la Recherche Scientifique, Université de Strasbourg, Institut des Neurosciences Cellulaires et Intégratives, 8 allée du Général Rouvillois, 67000 Strasbourg, France.

[3]Department of Biosciences and Territory, University of Molise, Contrada Fonte Lappone, 86090 Pesche, Italy.

[4]Neuroendocrinology Metabolism and Neuropharmacology Unit, IRCSS Fondazione Santa Lucia, Via del Fosso Fiorano 64, 00143 Rome, Italy.

*Co-corresponding and co-last authors: frank.pfrieger@unistra.fr; valentina.pallottini@uniroma3.it

Abstract

Niemann-Pick type C disease (NPCD) is a lysosomal disorder whith patients presenting highly variable onset, neurovisceral symptoms and life spans due to defective lipid homeostasis. At present, therapeutic options are limited to palliative and disease-modifying drugs, and there is a continued need for new approaches. Here, we explored bromodomain and extraterminal (BET) proteins as new drug target for NPCD using patient-derived fibroblasts. Treatment of cells with JQ1, a prototype BET inhibitor, enhanced the level of NPC1 protein and increased its presence in lysosomes, diminished lysosomal expansion and cholesterol accumulation and induced extracellular release of lysosomal components in a time- and dose-dependent manner. The reversal of pathologic changes in an established cell model suggest inhibition of BET protein as new therapeutic approach for NPCD.

Keywords: epigenetic regulation; lysosome; bromodomain; cholesterol; neurodegeneration; rare disease; proteostasis

Introduction

Niemann-Pick type C disease (NPCD) is a rare, autosomal-recessive, and pan-ethnic lysosomal disorder presenting progressive and ultimately fatal neurovisceral symptoms (Pfrieger, 2023; Vanier, 2010). The primary cause are specific variants of *NPC intracellular cholesterol transporter 1* (*NPC1*; OMIM #257220; 95% of cases) (Carstea et al., 1997; Loftus, 1997) or of *NPC intracellular cholesterol transporter 2* (*NPC2*; OMIM 607625; 5% of cases) (Naureckiene et al., 2000). The encoded proteins NPC1 and NPC2, which are ubiquitously expressed, reside in the membrane (Higgins et al., 1999; Kobayashi et al., 1999; Neufeld et al., 1999) and lumen of late endosomes (Blom et al., 2003; Naureckiene et al., 2000; Zhang et al., 2003), respectively. Genetic manipulations (Sleat et al., 2004), biochemical assays (Infante et al., 2008; Liou et al., 2006) and structure analyses (Friedland et al., 2003; Kwon et al., 2009; Li et al., 2016; Qian et al., 2020; Wang et al., 2016; Winkler et al., 2019) indicate that the two proteins mediate cooperatively the egress of unesterified cholesterol from the endosomal-lysosomal system.

Dysfunction of either protein causes intracellular accumulation of unesterified cholesterol (Pentchev et al., 1985; Vanier et al., 1991) and other lipids (Altuzar et al., 2023; Fan et al., 2013; Lloyd-Evans et al., 2008; Malathi et al., 2004; Sugimoto et al., 2001; Taniguchi et al., 2001; te Vruchte et al., 2004; Zervas et al., 2001a), and impairs lysosomal (Elrick et al., 2012; Ko et al., 2001; Lloyd-Evans et al., 2008; Shen et al., 2012; Zhang et al., 2001) and mitochondrial function (Colaco et al., 2020; Li et al., 2005; Marí et al., 2006; Torres et al., 2017; Yambire et al., 2019; Yu et al., 2005), and autophagy (Ko et al., 2005; Liao et al., 2007; Pacheco et al., 2007). Patients present distinct forms of the disease depending on the onset of neurovisceral symptoms (Bolton et al., 2022; Geberhiwot et al., 2018; Patterson, 2020; Rangel et al., 2020). The most common forms are characterized by infantile onset at two months to six years of age presenting hepatosplenomegaly, delayed motor and speech development, and progressive neurologic symptoms including dysphagia, ataxia, clumsiness, seizures, and cataplexy. These patients die within several years often due to respiratory failure (Pineda

et al., 2019; Yilmaz et al., 2020). The estimated incidence of NPCD is 1:100,000 births (Vanier, 2010) although the number of patients with the adolescent/adult form is probably higher (Wassif et al., 2016) due to lack of proper diagnosis.

Therapeutic options are still limited to treatment of specific symptoms like for example seizures, and to the disease-modifying N-butyl-deoxynojirimycin (OGT918, Miglustat, Zavesca) that inhibits glucosylceramide synthase (Platt et al., 1994) and non-lysosomal glucosylceramidase (GBA2) (Nietupski et al., 2012). The drug, which is approved for NPCD in many countries, but not in the US, slows down disease progression in NPC1-deficient mice (Zervas et al., 2001b), cats (Stein et al., 2012), and patients (Patterson et al., 2020; Patterson et al., 2007; Pineda et al., 2018; Solomon et al., 2022) except for those presenting early infantile disease onset (Freihuber et al., 2023). Within the last decade, numerous therapeutic approaches have been tested, but only few have entered clinical studies, and none has been approved (Bremova-Ertl and Schneider, 2023; Cariati et al., 2021; Heras et al., 2023; Pfrieger, 2023; Sitarska et al., 2021). Therefore, there is a strong need to develop new therapeutic approaches.

Here, we explored bromodomain and extra-terminal (BET) proteins as new drug target for NPCD. BET proteins bind to acetylated lysine on histones and thereby regulate gene transcription (Filippakopoulos and Knapp, 2014). They serve as therapeutic drug targets (Cochran et al., 2019) for different types of cancer (Shorstova et al., 2021) and many other pathologic conditions (Kulikowski et al., 2021; Martella et al., 2023) including cachexia (Segatto et al., 2017), Duchenne muscular dystrophy (Segatto et al., 2020), Fabry disease (Fu et al., 2022) and retinal inflammation due to STING activation (Zou et al., 2022), which also contributes to neurodegeneration in NPCD (Chu et al., 2021). Recently, we discovered that JQ1, a well-characterized competitive inhibitor of BET proteins (Filippakopoulos et al., 2010), enhances the protein content of NPC1 in cultured cells (Tonini et al., 2020). This effect has therapeutic potential for NPCD patients because disease severity correlates with cellular levels of NPC1 protein (Millat et al., 2001; Musalkova et al., 2020; Yamamoto et al., 2000) and because some pathogenic variants of NPC1 are functional, but degraded due to misfolding (Feng et al., 2019; Gelsthorpe et al., 2008; Macías-Vidal et al., 2014; Praggastis et al., 2015; Schultz et al., 2018; Wang et al., 2019).

Using patient-derived skin fibroblasts serving as established in vitro model for preclinical studies (Pallottini and Pfrieger, 2020) we show that inhibition of BET proteins increases the levels of NPC1 and its localization in the endosomal-lysosomal system, and reverts pathologic changes at least in part through lysosomal exocytosis. Together, our results suggest BET protein inhibition as a potential new therapeutic approach for NPCD.

Material and Methods

Cell culture and drug treatment

Dermal fibroblasts from a NPCD patient (GM18453) homozygous for a frequent pathogenic allele encoding the I1061T variant (Millat et al., 1999) and from a sex- and age-matched healthy donor (GM05659; NIGMS Human Genetic Cell Repository; Coriell Institute for Medical Research, Camden, NJ, USA) were cultured in Dulbecco's modified Eagle medium (DMEM) containing high glucose supplemented with 5% fetal bovine serum (FBS), 1% L-glutamine, 1% sodium pyruvate, 1% non-essential amino acids, and 1% penicillin-streptomycin (all Sigma-Aldrich/Merck) at 37°C and 5% CO_2. All experiments were performed at 60–70% cell confluency and maximally 20 passages. The drug (+)-JQ1 (#SML1524, Sigma-Aldrich/Merck) was added to primary cultures at indicated concentrations after dilution from a stock solution (3 mM in DMSO; stored at -20°C). Controls were treated with vehicle alone (0.1% DMSO in DMEM).

Cell numbers and viability

Fibroblasts were cultured in 24-well plates (#833922, Sarstedt) at 15,000 cells/well and treated as indicated. Cells were detached with trypsine/EDTA (0.05%), resuspended in medium, stained with propidium iodide (2 µg/ml; Sigma-Aldrich/Merck) to label dead cells, and subjected to flow cytometry (CytoFlex, Beckman Coulter) counting all cells and propidium iodide-positive cells (excitation at 488 nm, emission 585/42 band pass filter).

Lysate preparation and immunoblotting

Fibroblasts were cultured in 6-well plates at 150,000 cells/well and treated as indicated. Cells were lysed in homogenization buffer (Sucrose 0.1M, KCl 0.05M, KH_2PO_4 0.04M, EDTA 0.04M, pH 7.4, with protease inhibitor cocktail (1:1,000) and phosphatase inhibitor cocktail (1:400; Sigma-Aldrich/Merck) by sonication (VCX 130 PB, Sonics Materials) on ice for 20 sec. Samples were then centrifugated at 13,000 rpm for 10 min at 4°C to remove cell debris. Protein concentration was assessed by the Lowry method. For immunoblotting, samples were diluted with Laemmli buffer, boiled for 5 min, and subjected to SDS-PAGE (40 µg of protein/lane). Proteins were transferred to nitrocellulose membranes (Trans-Blot Turbo Transfer System; Bio-Rad Laboratories). Membranes were blocked with fat-free milk (5% in Tris-buffered saline 0.138M NaCl, 0.027M KCl, 0.025M Tris-HCl, and 0.05% Tween-20, pH 6.8) for 1h at room temperature (RT), exposed to antibodies against NPC1 (1:1,000; #NB400-148, Novus Biologicals) or vinculin (VCL) as loading control (1:40,000; #V9131, Sigma-Aldrich) overnight at 4°C followed by horseradish peroxidase-conjugated secondary IgG antibody (Bio-Rad Laboratories) for 1h at RT. Chemiluminescence was visualized using the ChemiDoc MP system (Bio-Rad Laboratories) and analyzed by ImageJ (National Institutes of Health, Bethesda, MD, USA).

Endoglycosidase H Assay

Fibroblasts were cultured in 6-well plates and treated as indicated. Cells were lysed in homogenization buffer (Sucrose 0.1M, KCl 0.05M, KH_2PO_4 0.04M, EDTA 0.04M, pH 7.4) by sonication (VCX 130 PB, Sonics Materials) at 4°C for 20 sec, and centrifuged at 12,000 rpm for 10 min at 4°C to yield total lysate. The endoglycosidase H (EndoH) assay (V4875, Promega) was performed following the manufacturer's instructions. The samples contained EndoH reaction buffer, water, and EndoH enzyme, for negative controls, the EndoH enzyme was replaced by water. All samples were incubated at 37°C for 6 hours, and the reaction was terminated by adding Laemmli sample buffer before immunoblotting.

Immunocytochemical staining

Fibroblasts were cultured on 96-well microplates (black imaging plate; #353219, BD Falcon, Becton-Dickinson) at 3,000 cells/well and treated as indicated. Cells were washed three times with phosphate-buffered saline (PBS), and fixed with 4% paraformaldehyde (in PBS) for 15 min at RT. Cells were permeabilized (0.05% Saponin in PBS) for 10 min, and incubated for 45 min with blocking solution (3% BSA with 1% goat serum in PBS) and then overnight at 4°C with primary antibodies (1% BSA in PBS) against NPC1 (1:2,500; NB400-148, Novus Biologicals) and LAMP2 (1:1,000; #sc-18822, Santa-Cruz). After incubation, cells were washed and reacted for 1h at RT with appropriate secondary antibodies (1:1,000; goat anti-rabbit secondary antibody Alexa Fluor 546; #A-10040, ThermoFisher Scientific; goat anti-mouse secondary antibody Alexa Fluor 488; #A-11001, ThermoFisher Scientific). Fluorescence was visualized and digitized using an upright microscope (Zeiss Observer 7) equipped with a light source (Zeiss Colibri), objectives (40x water, N.A. 1.2; 63x oil, N.A. 1.4; Zeiss), a module for optical sectioning by structured illumination (Zeiss ApoTome.2) and a digital camera (Hamamatsu ORCA-Flash 4.0). Colocalization analysis was performed using ImageJ and the plugin JaCoP (Just another Colocalization Plugin) to measure Pearson's correlation coefficients in manually selected regions of interest.

Cytochemical staining

Fibroblasts were cultured on 96-well microplates (black imaging plate; #353219, BD Falcon) at 3,000 cells/well and treated as indicated. Cells were washed three times with PBS, fixed by paraformaldehyde (4% in PBS) for 15 min at RT and stained with filipin (50 µg/mL in PBS prepared freshly from a 250-fold ethanolic stock; #F9765, Sigma-Aldrich/Merck) for 2h at RT in the dark. Fluorescence images of stained cells were acquired using an inverted microscope (Axiovert 135TV; Zeiss) equipped with a metal halide lamp (10%; Lumen 200; Prior Scientific), an appropriate excitation/emission filter (XF02-2; Omega Optical Inc.), a 40x objective (oil, N.A. 1.3; Zeiss) and an air-cooled monochrome charge-coupled device camera (Sensicam, PCO Computer Optics) controlled by custom-written Labview routines (National Instruments). Density of filipin-positive puncta was

determined in manually outlined somata using custome-written Labview routines (Demais et al., 2016).

Lysotracker staining and cytometry

Fibroblasts were cultured in 6-well plates (#833920 Sarstedt) at 150,000 cells/wells and treated as indicated. Before the end of the treatment, cells were incubated with LysoTracker Red DND-99 (1 µM in culture medium; #L7528, Life technologies) for 30 minutes at 37°C, detached, spun-down at 13,000 rpm and resuspended in 300 µL of medium prior to flow cytometry. Data were acquired using a flow cytometer (Cytoflex-LX; Bekman-Coulter) and analyzed by specialized software (Kaluza, Beckman Coulter; FloJo, Becton-Dickinson). Fold-changes in LysoTracker intensity were calculated as ratios of geometric means of stained / unstained samples as described (Rodriguez-Gil et al., 2013).

Hexosaminidase activity assay

Cells were cultured in 96-well microplates source (#833924, Sarstedt) at 4,000 cells/wells in DMEM without phenol red. The assay was performed similar as described (Demais et al., 2016). Briefly, at the end of the treatment, 20 µL of cell culture medium were incubated at 37°C for 3 hours with 20 µL reaction mix containing sodium citrate (10 mM; pH 4.2) and 4-methylumbelliferyl-2-acetamido-2-deoxy-b-D-glucopyranoside (2 mM; #474502, Sigma-Aldrich/Merck). The reaction was stopped by 5 volumes of glycine and Na_2CO_3. (0.2M). Crystal violet (#C0775, Sigma-Aldrich/Merck; 0.05% in H_2O with 1% paraformaldehyde and 1% methanol) was added to the cell suspension to indicate cell number. The fluorescent product 4-methylumbelliferone and crystal violet were measured in triplicate on a microplate reader (Tecan Spark, Männedorf, Switzerland) using suitable filters (excitation: 365 nm; emission filters: 440 nm; absorbance: 585 nm). Calibration curves were acquired using defined amounts of the fluorescent product 4-methylumbelliferone sodium salt (#M1508, Sigma-Aldrich/Merck). Fluorescence of 4-methylumbelliferone was normalized to crystal violet intensity.

Data analysis and visualisation

Data analysis and visualisation were accomplished with the open source software R (R Core Team, 2021) and selected packages (data.table, ggplot2). Unless indicated otherwise, results are displayed using bar and whisker plots representing mean and standard deviation, respectively. Statistical tests were performed as indicated. When comparing three or more experimental groups, analysis of variance (ANOVA) was carried out, followed by Tukey's post-hoc test. Asterisks indicate statistically significant differences based on p values (*, $p < 0.05$; **, $p < 0.01$; ***, $p < 0.001$).

Results

Here we explored whether BET proteins can serve as new therapeutic target for NPCD using the membrane-permeant inhibitor JQ1 and primary cultures of human dermal fibroblasts from NPCD patients.

Effects of JQ1 on viability, protein levels of NPC1 and its distribution in fibroblasts

First, we tested whether the drug affected the number and viability of dermal fibroblasts. As shown in Fig. 1A, patient-derived fibroblasts carrying the I1061T variant attained lower numbers at each time point tested, and showed a lower fraction of propidium-iodide-positive (dead) cells compared to fibroblasts with normal NPC1. JQ1 inhibited cell growth compared to vehicle (DMSO) (Fig. 1B) as reported previously in dermal fibroblasts (Vichaikul et al., 2022) and in immortalized cell lines (Filippakopoulos et al., 2010). This effect occurred regardless of the genotype (Fig. 1B). The drug enhanced the percentage of dead cells at 48h of treatment in healthy fibroblasts, but the most robust effects occurred in patient-derived cells after 96h of treatment (Fig. 1B).

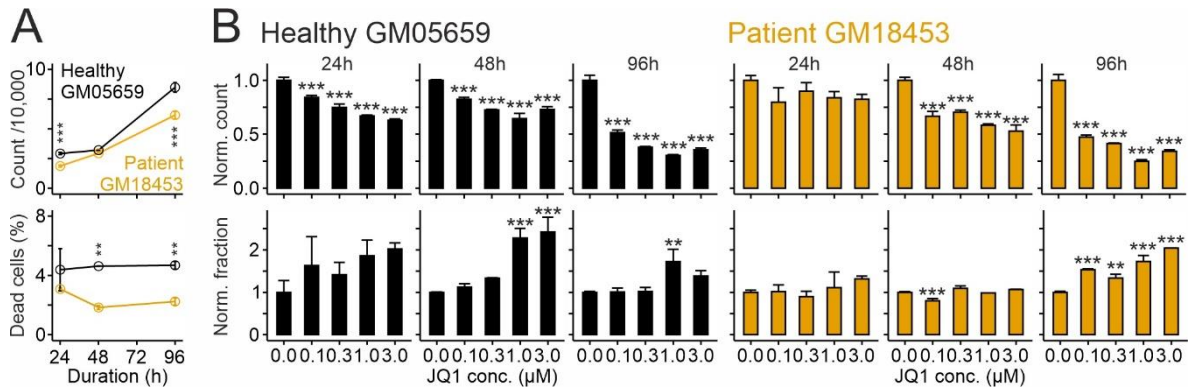

Figure 1. Effects of JQ1 on cell numbers and viability in primary cultures of human skin fibroblasts.

Cell counts (top) and percentages of propidium iodide-positive cells (bottom) in primary cultures of skin fibroblasts from a healthy donor (GM056549; black) and a NPCD patient (GM018453; orange) in untreated cells (A) and after treatment with JQ1 or vehicle (DMSO) for indicated periods and concentrations (B). Values in B were normalized to values from vehicle-treated control cultures run in parallel. Asterisks indicate statistically significant changes (ANOVA with Tukey's post-hoc test; n = 3 independent preparations for each experiment).

Next, we tested how JQ1 affects the level of NPC1 protein in human fibroblasts. These experiments followed up on our observation that the drug modifies components mediating lipid homeostasis including NPC1 in a hepatocarcinoma cell line (Tonini et al., 2020). Immunoblotting revealed lower levels of the I1061T variant compared to the normal version of NPC1 in fibroblasts (Fig. 2A) in agreement with previous studies (Gelsthorpe et al., 2008; Pipalia et al., 2011; Yu et al., 2012). Treatment with JQ1 enhanced the levels of NPC1 in a concentration-dependent manner compared to vehicle-treated cultures independently from the genotype with statistically significant changes occurring after 72h of treatment (Fig. 2B). The fraction of EndoH-resistant NPC1 variant was unaffected by JQ1 (Fig. 2C) indicating that JQ1 does not impede protein glycosylation in the Golgi apparatus.

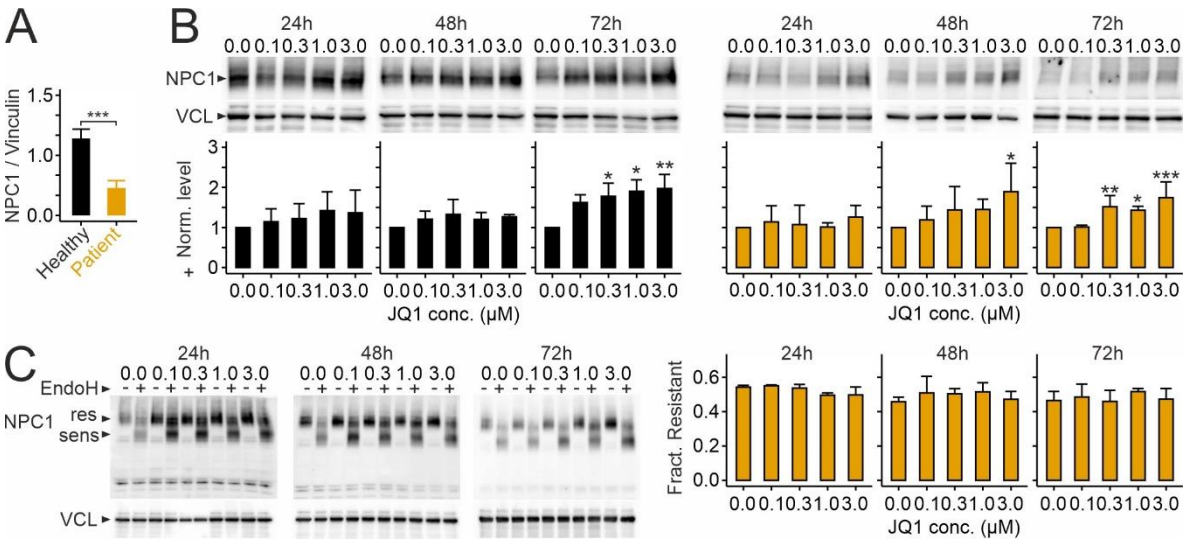

Figure 2. JQ1 enhances NPC1 protein levels in cultured skin fibroblasts.

Levels of NPC1 protein in primary cultures of skin fibroblasts from a healthy donor (GM056549; black) and a NPCD patient (GM018453; orange) in untreated cells (A) and after treatment with JQ1 or vehicle (DMSO) for indicated periods and concentrations (B). Values in A and B were normalized to vinculin (VCL) levels and to vehicle-treated control cultures, respectively. Asterisks indicate statistically significant changes (A: t test; n = 4 preparations; B: ANOVA with Tukey's post-hoc test; n = 3–7 preparations). C, Fraction of EndoH-resistant protein compared to total protein in patient-derived fibroblasts after treatment with JQ1 as indicated (n = 3 preparations per treatment). Note the change in protein size following EndoH-mediated glycan removal. Images in (B) and (C) show representative immunoblots reacted with antibodies against NPC1 and VCL as loading control.

Next, we asked whether JQ1-induced NPC1 protein reaches the endosomal-lysosomal system using double immunocytochemical staining with antibodies against NPC1 and against the endosomal-lysosomal marker LAMP2 (Fig. 3A). Quantitative analyses confirmed lower levels of marker colocalization in patient-derived fibroblasts compared to the health control cells (Fig. 3B). Treatment of patient-derived cells with JQ1 enhanced the colocalization of NPC1 with LAMP2 (Fig. 3C).

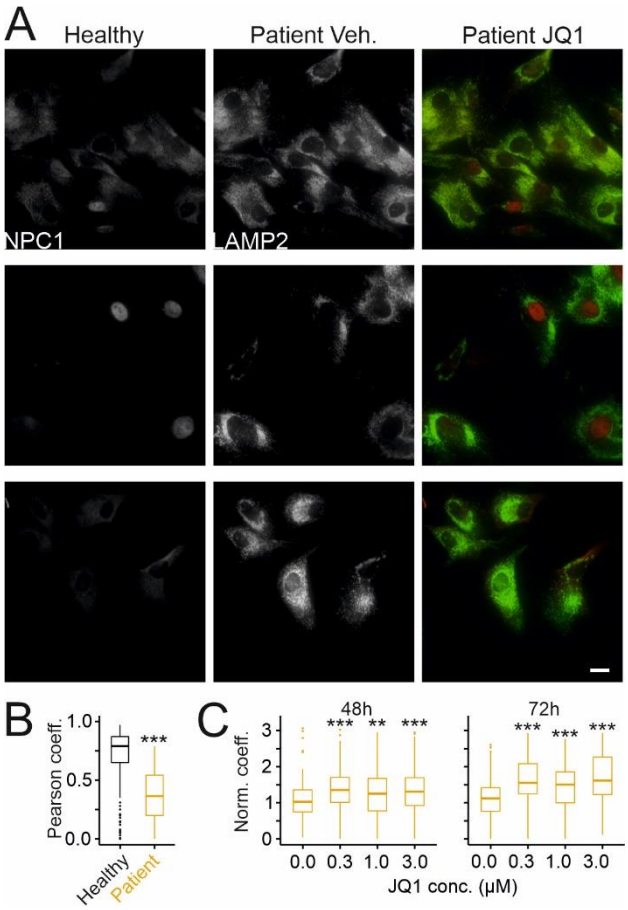

Figure 3. JQ1 enhances presence of NPC1 in the endosomal-lysosomal system.

A, Fluorescence micrographs of cultured fibroblasts from a healthy donor (top) and a NPCD patient following treatment for 72h with vehicle or JQ1. Cells were fixed and subjected to immunocytochemical staining for NPC1 and LAMP2. False-color micrographs represent overlays of NPC1 (red) and LAMP2 (green). Scale bar: 20 µm. B, C Boxplots showing Pearson's correlation coefficients of NPC1 and LAMP2 intensity in somata of fibroblasts without treatment (B), and in patient-derived fibroblasts following treatment with JQ1 as indicated (C). In C, coefficients were normalized to the means of vehicle-treated cultures. Asterisks indicate statistically significant changes (B: t test; n = 185/171 healthy/patient cells, 4 preparations; C: ANOVA with Tukey's post-hoc test; n = 99–162 cells per treatment, 4 preparations).

JQ1-induced effects on pathologic changes in patient-derived fibroblasts

Since JQ1 increased the endosomal-lysosomal level of NPC1 protein, we tested whether the drug reverts hallmarks of NPC1-deficiency in these cells, the accumulation of unesterified cholesterol and the expansion of the acidic (lysosomal) compartments, using cytochemical staining with the cholesterol-binding drug filipin (Pentchev et al., 1985) and a pH-sensitive fluorescent dye named lysotracker (Funk and Krise, 2012; Rodriguez-Gil et al., 2013; te Vruchte et al., 2014; Xu et al., 2014), respectively (Fig. 4). As expected based on previous studies, patient-derived fibroblasts showed a higher density of filipin-positive puncta (Fig. 4A, B), larger cell complexity and stronger lysotracker fluorescence compared to cells from the healthy donor (Fig. 4D-F). Surprisingly, JQ1 increased the density of filipin-positive puncta after 48h of treatment (Fig. 4C). Treatment for 72h seemed to lack an effects on filipin densities (Fig. 4C). However, at closer inspection we observed a dual effect with some cells showing an increase, whereas others showed no change or a decrease of filipin densities after this treatment duration (Fig. 4A, C, insert). This finding suggested a time-dependent switch of the JQ1 effect. To test this possibility, we treated cells with JQ1 for 168h. This prolonged treatment period reduced the accumulation of cholesterol in patient-derived fibroblasts already at the lowest dose tested (Figs. 4C). Flow cytometry of lysotracker-labeled cells confirmed that cells bearing the disease-causing variant of NPC1 had a larger acidic compartment than cells from a healthy donor (Fig. 4D–F). Notably, treatment of patient-derived cells with JQ1 reduced this compartment in a dose-dependent manner at all time points tested (Fig. 4G).

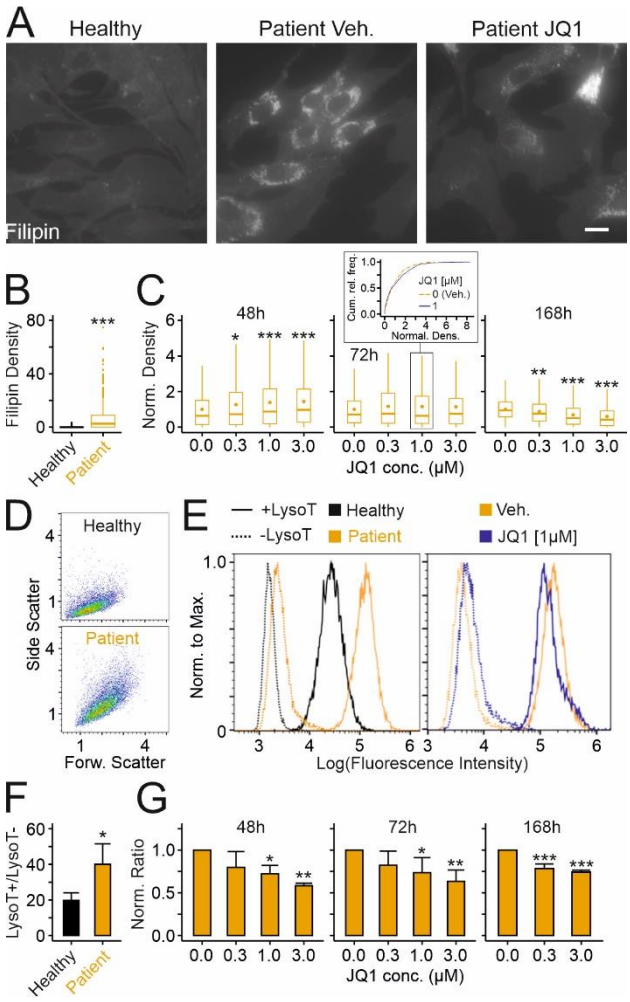

Figure 4. JQ1 reverts pathologic lysosomal changes in patient-derived fibroblasts.

A, Fluorescence micrographs showing cultured fibroblasts from a healthy donor and a NPCD patient following treatment for 72h with JQ1 (3 µM) or vehicle (Veh.; DMSO). Cells were fixed and subjected to cytochemical staining with filipin to reveal the distribution of unesterified cholesterol. Scale bar: 20 µm. B, Boxplots showing densities of filipin-positive puncta in fibroblasts from a healthy donor and from NPCD patient. C, Boxplots showing densities of filipin-positive puncta normalized to the means of vehicle-treated cultures following treatment with JQ1 for indicated durations and concentrations. Circles indicate mean values. Insert, cumulative relative frequency distributions of filipin densities in cells treated for 72h with JQ1 (1µM) or with vehicle (0 µM). Note the dual effect of JQ1 inducing a increase and a small decrease of cholesterol accumulation at this time point. Asterisks indicate statistically significant changes (B: t test; n = 502/608 healthy/patient-

derived cells from 4 preparations; C: ANOVA with Tukey's post-hoc test; 48h: 434–479 cells per treatment, 3 preparations; 72h: n = 390–527 cells per treatment, 3 preparations; 168h: n = 453–818 cells, 5 preparations). D, Representative plots of side and forward scatter intensities. E, Histograms of fluorescence intensities normalized to maxima in cells from indicated donors untreated or treated with JQ1 and unstained or stained with lysotracker as indicated. F, G, Mean ratios of geometric means (lysotracker signal divided by background signal from cells without lysotracker) in fibroblasts without treatment (F), and in patient-derived fibroblasts following treatment with JQ1 (G) as indicated. In G, ratios were normalized to the means of vehicle-treated (concentration 0) cultures (B: t test; n = 4 preparations; C: ANOVA with Tukey's post-hoc test; n = 3–5 preparations.

JQ-induced lysosomal exocytosis

The reduction of the lysotracker signal raised the question whether JQ1 enhanced the release of lysosomal content to the extracellular medium. To address this point, we performed two complementary assays, namely immunocytochemical staining of LAMP2 on the surface of non-permeabilized cells and detection of hexosaminidase activity in the culture medium (Fig. 5). Both assays revealed that NPC1 deficiency enhances basal LAMP2 surface expression (Fig 5A, B) and hexosaminidase activity (Fig. 5D) in patient-derived fibroblasts compared to normal cells. Treatment with JQ1 increased both the surface expression (Fig. 5C) and hexosaminidase release in a concentration-dependent manner (Fig. 5E) suggesting that the drug induces release of lysosomal material.

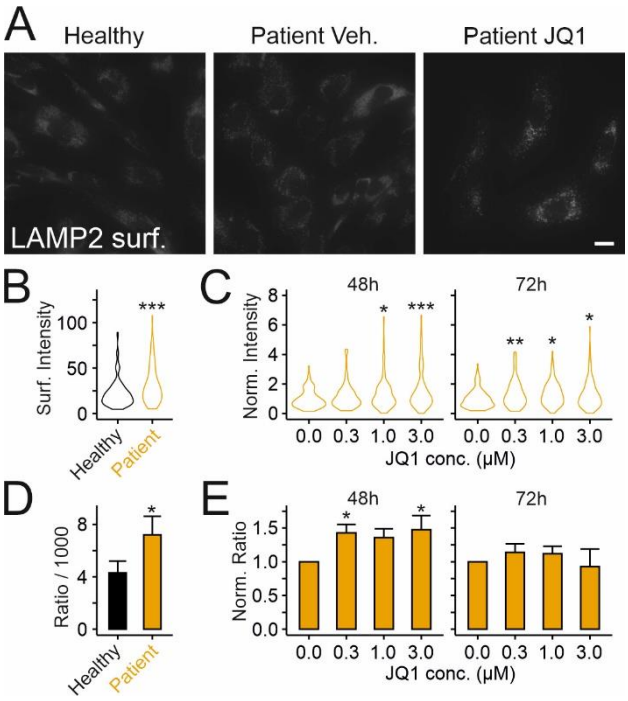

Figure 5. JQ1 induces extracellular release of lysosomal material in patient-derived fibroblasts. A, Fluorescence micrographs showing cultured fibroblasts from a healthy donor and a NPCD patient following treatment for 72h with JQ1 or vehicle (Veh.). Cells were fixed without permeabilization and subjected to immunocytochemical staining to reveal the surface distribution of LAMP2. Scale bar: 20 µm. B, C, Violinplots showing fluorescence intensities indicating surface expression of LAMP2 on somata of fibroblasts without treatment (B), and in patient-derived fibroblasts following treatment with JQ1 as indicated (C). In C, intensities were normalized to the means of vehicle-treated cultures. Black points indicate means. Asterisks indicate statistically significant changes (B: t test; n = 153/131 healthy/patient-derived cells from 4 preparations; C: ANOVA with Tukey's post-hoc test; 48h: 85–116; 72h: n = 102–131 cells per treatment from 3–4 preparations). D, E, Hexosaminidase activity normalized to cell numbers in fibroblasts without treatment (D), and in patient-derived fibroblasts following treatment with JQ1 as indicated (E). In E, values were normalized to the means of vehicle-treated (concentration 0) cultures (D: t test; n = 3–4 preparations; E: ANOVA with Tukey's post-hoc test; n = 3–4 preparations).

Discussion

Our work identifies inhibitors of BET proteins as new drug candidates for NPCD. This is based on our observations that a prototypic inhibitor enhanced the level of NPC1 protein and increased its presence in lysosomes, diminished lysosomal expansion and cholesterol accumulation, and induced release of lysosomal components in a time- and dose-dependent manner.

Our finding that BET protein inhibition enhances NPC1 protein as a component of the endosomal-lysosomal system is in line with previous reports that the promoter region of *Npc1* is associated with acetylated histones (Gevry et al., 2003) and that de-acetylation increases gene expression (Munkacsi et al., 2011). More generally, BET proteins have been shown to control lysosome- and autophagy-related genes in various cell types and disease conditions (Campbell et al., 2018; Gong et al., 2022; Jang et al., 2017; Li et al., 2020; Sakamaki et al., 2017; Segatto et al., 2020; Shen et al., 2020; Sui et al., 2019; Wakita et al., 2020). Other pathways to enhance cellular NPC1 protein levels have been explored *in vitro* including inhibition of histone deacetylases (Newton et al., 2017; Nunes et al., 2013; Pipalia et al., 2011; Pipalia et al., 2017; Praggastis et al., 2015; Wang et al., 2019), enhanced chaperone activity (Gelsthorpe et al., 2008; Nakasone et al., 2014; Ohgane et al., 2013; Pipalia et al., 2021; Schultz et al., 2022; Völkner et al., 2022; Wang et al., 2020; Yu et al., 2012; Zampieri et al., 2012) and reduced protein degradation (Gelsthorpe et al., 2008; Macías-Vidal et al., 2014; Nakasone et al., 2014; Zampieri et al., 2012). Similar to what we observed following JQ1 treatment, these manipulations enhanced the presence of NPC1 variants in the endosomal-lysosomal system (Gelsthorpe et al., 2008; Macías-Vidal et al., 2014; Ohgane et al., 2013; Pipalia et al., 2021; Pipalia et al., 2017; Völkner et al., 2022; Wang et al., 2019; Wang et al., 2020; Yu et al., 2012; Zampieri et al., 2012) and decreased the intracellular accumulation of unesterified cholesterol (Gelsthorpe et al., 2008; Macías-Vidal et al., 2014; Munkacsi et al., 2011; Newton et al., 2017; Ohgane et al., 2013; Pipalia et al., 2011; Pipalia et al., 2021; Pipalia et al., 2017; Praggastis et al., 2015; Völkner et al., 2022; Wang et al., 2019; Wehrmann et al., 2012; Yu et al., 2012; Zampieri et al., 2012). Interestingly, however, these manipulations reverted cholesterol accumulation within maximally 72h, whereas JQ1 affected cholesterol levels at a slower pace. In this context, we note a recent fibroblast-based high-throughput drug screen for NPCD, which revealed an effect of JQ1 on

LAMP1 levels, but not on cholesterol accumulation (Pugach et al., 2018). Our results posit that this apparent lack of effect was due to the 72h time window selected for this assay. In fact, our study reveals a biphasic effect of JQ1. The transient cholesterol accumulation within 48h may be due to enhanced autophagy and lysosome function as reported previously (Sakamaki et al., 2017). The concomitant reduction of the lysosomal volume as indicated by lysotracker staining may at least in part be caused by release of lysosomal content to the extracellular space. Evidence for induction of this pathway by JQ1 is based on the enhanced presence of LAMP2 on the cell surface and increased hexosaminidase activity in the medium. This pathway may also limit the extent of cholesterol accumulation due to NPC1 dysfunction as suggested by previous studies on cell lines (Chen et al., 2010; Feltes et al., 2020; Vacca et al., 2019), patient-derived fibroblasts (Arguello et al., 2021; Cao et al., 2015; Xu et al., 2012), and retinal neurons in vitro (Demais et al., 2016) and in vivo (Barthelemy et al., 2021).

The protracted decrease of cholesterol accumulation over 7 days may be due to the lower efficacy of the I1061T NPCD variant to export cholesterol from the endosomal-lysosomal system. The delay may also be caused by a sequence of changes in pathways or processes that are affected by BET protein inhibition (Garcia et al., 2023). Obvious candidates based on previous studies are a reduction of cholesterol biosynthesis (Shen et al., 2021; Tonini et al., 2020) and of intracellular lipid levels (Tonini et al., 2020) and an increase of apolipoprotein a (McLure et al., 2014), which has been explored as therapeutic agent for NPCD (Schultz et al., 2019). In general, BET protein inhibition affects many transcriptional programs through interactions with acetylated lysins on histones including a site showing epigenetic marks in NPCD (Kunkel et al., 2023).

<u>Conflict of Interest</u>

MS and VP are listed as inventors on an Italian patent related to the therapeutic use of BET proteins.

Funding

The authors gratefully acknowledge support by the Ara Parseghian Medical Research Fund (MS, FWP), BILD hilft e.V. (FWP), Niemann-Pick Selbsthilfegruppe e.V. (FWP, VP), Telethon Italy (VP), and Together Strong Niemann-Pick foundation (VP).

Author contributions

Conceptualization: AS, CT, FWP, MP, MS, VP; Data curation: AB, AS, FWP, MP, VP; Formal Analysis: AB, AS, CT, FWP, MP, VP; Funding acquisition: FWP, MS, VP; Investigation: AB, AS, CT, LS, MP; Methodology: AB, AS, CT, FWP, LS, MP, VP; Project administration: AB, CT, FWP, MP, VP. Resources: AS, FWP, VP; Software: AS, FWP; Supervision: FWP, VP; Validation: AB, FWP, MP, VP; Visualization: AS, FWP, VP; Writing – original draft: FWP; Writing – review & editing: AB, AS, FWP, MP, MS, VP.

References

Altuzar, J., et al. (2023) Lysosome-targeted multifunctional lipid probes reveal the sterol transporter NPC1 as a sphingosine interactor. Proc Natl Acad Sci USA 120: e2213886120. https://doi.org/10.1073/pnas.2213886120.

Arguello, G., et al. (2021) Genistein Activates Transcription Factor EB and Corrects Niemann-Pick C Phenotype. Int J Mol Sci 22: https://doi.org/10.3390/ijms22084220.

Barthelemy, A., et al. (2021) Glial contribution to cyclodextrin-mediated reversal of cholesterol accumulation in murine NPC1-deficient neurons in vivo. Neurobiol Dis 158: 105469. https://doi.org/https://doi.org/10.1016/j.nbd.2021.105469.

Blom, T. S., et al. (2003) Defective endocytic trafficking of NPC1 and NPC2 underlying infantile Niemann-Pick type C disease. Hum Mol Genet 12: 257-272. https://doi.org/10.1093/hmg/ddg025.

Bolton, S. C., et al. (2022) Clinical disease characteristics of patients with Niemann-Pick Disease Type C: findings from the International Niemann-Pick Disease Registry (INPDR). Orphanet J Rare Dis 17: https://doi.org/10.1186/s13023-022-02200-4.

Bremova-Ertl, T., Schneider, S. (2023) Current advancements in therapy for Niemann-Pick disease: progress and pitfalls. Expert Opin Pharmacother 1-19. https://doi.org/10.1080/14656566.2023.2215386.

Campbell, G. R., et al. (2018) Induction of autophagy by PI3K/MTOR and PI3K/MTOR/BRD4 inhibitors suppresses HIV-1 replication. J Biol Chem 293: 5808-5820. https://doi.org/10.1074/jbc.RA118.002353.

Cao, Q., et al. (2015) BK Channels Alleviate Lysosomal Storage Diseases by Providing Positive Feedback Regulation of Lysosomal Ca2+ Release. Dev Cell 33: 427-441. https://doi.org/10.1016/j.devcel.2015.04.010.

Cariati, I., et al. (2021) Neurodegeneration in Niemann-Pick Type C Disease: An Updated Review on Pharmacological and Non-Pharmacological Approaches to Counteract Brain and Cognitive Impairment. Int J Mol Sci 22: https://doi.org/10.3390/ijms22126600.

Carstea, E. D., et al. (1997) Niemann-Pick C1 Disease Gene: Homology to Mediators of Cholesterol Homeostasis. Science 277: 228-231. https://doi.org/ 10.1126/science.277.5323.228.

Chen, F. W., et al. (2010) Cyclodextrin induces calcium-dependent lysosomal exocytosis. PLOS ONE 5: e15054. https://doi.org/10.1371/journal.pone.0015054.

Chu, T.-T., et al. (2021) Tonic prime-boost of STING signalling mediates Niemann–Pick disease type C. Nature 596: 570-575. https://doi.org/10.1038/s41586-021-03762-2.

Cochran, A. G., et al. (2019) Bromodomains: a new target class for drug development. Nat Rev Drug Discov 18: 609-628. https://doi.org/10.1038/s41573-019-0030-7.

Colaco, A., et al. (2020) Unbiased yeast screens identify cellular pathways affected in Niemann-Pick disease type C. Life Sci Alliance 3: https://doi.org/10.26508/lsa.201800253.

Demais, V., et al. (2016) Reversal of Pathologic Lipid Accumulation in NPC1-Deficient Neurons by Drug-Promoted Release of LAMP1-Coated Lamellar Inclusions. J. Neurosci. 36: 8012-8025. https://doi.org/10.1523/JNEUROSCI.0900-16.2016.

Elrick, M. J., et al. (2012) Impaired proteolysis underlies autophagic dysfunction in Niemann-Pick type C disease. Hum Mol Genet 21: 4876-4887. https://doi.org/10.1093/hmg/dds324.

Fan, M., et al. (2013) Identification of Niemann-Pick C1 disease biomarkers through sphingolipid profiling. J Lipid Res 54: 2800-2814. https://doi.org/10.1194/jlr.M040618.

Feltes, M., et al. (2020) Monitoring the itinerary of lysosomal cholesterol in Niemann-Pick Type C1-deficient cells after cyclodextrin treatment. J Lipid Res 61: 403-412. https://doi.org/10.1194/jlr.RA119000571.

Feng, X., et al. (2019) Determination of the Pathological Features of NPC1 Variants in a Cellular Complementation Test. Int J Mol Sci 20: 5185. https://doi.org/ 10.3390/ijms20205185.

Filippakopoulos, P., Knapp, S. (2014) Targeting bromodomains: epigenetic readers of lysine acetylation. Nat Rev Drug Discov 13: 339-358. https://doi.org/10.1038/nrd4286.

Filippakopoulos, P., et al. (2010) Selective inhibition of BET bromodomains. Nature 468: 1067-1073. https://doi.org/10.1038/nature09504.

Freihuber, C., et al. (2023) Effects of miglustat therapy on neurological disorder and survival in early-infantile Niemann-Pick disease type C: a national French retrospective study. Orphanet J Rare Dis 18: https://doi.org/10.1186/s13023-023-02804-4.

Friedland, N., et al. (2003) Structure of a Cholesterol-Binding Protein Deficient in Niemann-Pick Type C2 Disease. Proc Natl Acad Sci USA 100: 2512-2517. https://doi.org/10.1073/pnas.0437840100.

Fu, L., et al. (2022) Inhibition of epigenetic reader proteins by apabetalone counters inflammation in activated innate immune cells from Fabry disease patients receiving enzyme replacement therapy. Pharmacol Res Perspect 10: https://doi.org/10.1002/prp2.949.

Funk, R. S., Krise, J. P. (2012) Cationic amphiphilic drugs cause a marked expansion of apparent lysosomal volume: implications for an intracellular distribution-based drug interaction. Mol Pharm 9: 1384-1395. https://doi.org/10.1021/mp200641e.

Garcia, G., et al. (2023) Large-scale genetic screens identify BET-1 as a cytoskeleton regulator promoting actin function and life span. Aging Cell 22: e13742. https://doi.org/10.1111/acel.13742.

Geberhiwot, T., et al. (2018) Consensus clinical management guidelines for Niemann-Pick disease type C. Orphanet J Rare Dis 13: 50. https://doi.org/10.1186/s13023-018-0785-7.

Gelsthorpe, M. E., et al. (2008) Niemann-Pick type C1 I1061T mutant encodes a functional protein that is selected for endoplasmic reticulum-associated degradation due to protein misfolding. J Biol Chem 283: 8229-8236. https://doi.org/10.1074/jbc.M708735200.

Gevry, N. Y., et al. (2003) Regulation of Niemann-Pick C1 gene expression by the 3 ' 5 '-cyclic adenosine monophosphate pathway in steroidogenic cells. Mol Endocrinol 17: 704-715. https://doi.org/10.1210/me.2002-0093.

Gong, Z. G., et al. (2022) Epigenetic regulator BRD4 is involved in cadmium-induced acute kidney injury via contributing to lysosomal dysfunction, autophagy blockade and oxidative stress. Journal of Hazardous Materials 423: https://doi.org/10.1016/j.jhazmat.2021.127110.

Heras, M. L., et al. (2023) Understanding the phenotypic variability in Niemann-Pick disease type C (NPC): a need for precision medicine. Npj Genom Med 8: https://doi.org/10.1038/s41525-023-00365-w.

Higgins, M. E., et al. (1999) Niemann-Pick C1 is a late endosome-resident protein that transiently associates with lysosomes and the trans-Golgi network. Mol Genet Metab 68: 1-13. https://doi.org/10.1006/mgme.1999.2882.

Infante, R. E., et al. (2008) NPC2 facilitates bidirectional transfer of cholesterol between NPC1 and lipid bilayers, a step in cholesterol egress from lysosomes. Proc Natl Acad Sci USA 105: 15287-15292. https://doi.org/10.1073/pnas.0807328105.

Jang, J. E., et al. (2017) Targeting AMPK-ULK1-mediated autophagy for combating BET inhibitor resistance in acute myeloid leukemia stem cells. Autophagy 13: 761-762. https://doi.org/10.1080/15548627.2016.1278328.

Ko, D. C., et al. (2001) Dynamic movements of organelles containing Niemann-Pick C1 protein: NPC1 involvement in late endocytic events. Mol Biol Cell 12: 601-614. https://doi.org/10.1091/mbc.12.3.601.

Ko, D. C., et al. (2005) Cell-autonomous death of cerebellar purkinje neurons with autophagy in Niemann-Pick type C disease. PLoS Genet 1: 81-95. https://doi.org/10.1371/journal.pgen.0010007.

Kobayashi, T., et al. (1999) Late endosomal membranes rich in lysobisphosphatidic acid regulate cholesterol transport. Nat Cell Biol 1: 113-118. https://doi.org/10.1038/10084.

Kulikowski, E., et al. (2021) Inhibitors of bromodomain and extra-terminal proteins for treating multiple human diseases. Med Res Rev 41: 223-245. https://doi.org/10.1002/med.21730.

Kunkel, T. J., et al. (2023) The cholesterol transporter NPC1 is essential for epigenetic regulation and maturation of oligodendrocyte lineage cells. Nat Commun 14: 3964. https://doi.org/10.1038/s41467-023-39733-6.

Kwon, H. J., et al. (2009) Structure of N-terminal domain of NPC1 reveals distinct subdomains for binding and transfer of cholesterol. Cell 137: 1213-1224. https://doi.org/10.1016/j.cell.2009.03.049.

Li, H., et al. (2005) Molecular, anatomical, and biochemical events associated with neurodegeneration in mice with Niemann-Pick type C disease. J Neuropathol Exp Neurol 64: 323-333. https://doi.org/10.1093/jnen/64.4.323.

Li, X., et al. (2016) Clues to the mechanism of cholesterol transfer from the structure of NPC1 middle lumenal domain bound to NPC2. Proc Natl Acad Sci USA 113: 10079-10084. https://doi.org/10.1073/pnas.1611956113.

Li, Y., et al. (2020) Inhibition of Brd4 by JQ1 Promotes Functional Recovery From Spinal Cord Injury by Activating Autophagy. Front Cell Neurosci 14: 555591. https://doi.org/10.3389/fncel.2020.555591.

Liao, G., et al. (2007) Cholesterol accumulation is associated with lysosomal dysfunction and autophagic stress in Npc1 -/- mouse brain. Am J Pathol 171: 962-975. https://doi.org/10.2353/ajpath.2007.070052.

Liou, H. L., et al. (2006) NPC2, the protein deficient in Niemann-Pick C2 disease, consists of multiple glycoforms that bind a variety of sterols. J Biol Chem 281: 36710-36723. https://doi.org/10.1074/jbc.M608743200.

Lloyd-Evans, E., et al. (2008) Niemann-Pick disease type C1 is a sphingosine storage disease that causes deregulation of lysosomal calcium. Nat Med 14: 1247-1255. https://doi.org/10.1038/nm.1876.

Loftus, S. K. (1997) Murine Model of Niemann-Pick C Disease: Mutation in a Cholesterol Homeostasis Gene. Science 277: 232-235. https://doi.org/10.1126/science.277.5323.232.

Macías-Vidal, J., et al. (2014) The proteasome inhibitor bortezomib reduced cholesterol accumulation in fibroblasts from Niemann-Pick type C patients carrying missense mutations. FEBS J 281: 4450-4466. https://doi.org/10.1111/febs.12954.

Malathi, K., et al. (2004) Mutagenesis of the putative sterol-sensing domain of yeast Niemann Pick C-related protein reveals a primordial role in subcellular sphingolipid distribution. J Cell Biol 164: 547-556. https://doi.org/10.1083/jcb.200310046.

Marí, M., et al. (2006) Mitochondrial free cholesterol loading sensitizes to TNF- and Fas-mediated steatohepatitis. Cell Metab 4: 185-198. https://doi.org/https://doi.org/10.1016/j.cmet.2006.07.006.

Martella, N., et al. (2023) Bromodomain and Extra-Terminal Proteins in Brain Physiology and Pathology: BET-ing on Epigenetic Regulation. Biomedicines 11: https://doi.org/10.3390/biomedicines11030750.

McLure, K. G., et al. (2014) RVX-208, an Inducer of ApoA-I in Humans, Is a BET Bromodomain Antagonist. PLOS ONE 8: e83190. https://doi.org/10.1371/journal.pone.0083190.

Millat, G., et al. (1999) Niemann-Pick C1 disease: the I1061T substitution is a frequent mutant allele in patients of Western European descent and correlates with a classic juvenile phenotype. Am J Hum Genet 65: 1321-1329. https://doi.org/10.1086/302626.

Millat, G., et al. (2001) Niemann-Pick C1 disease: correlations between NPC1 mutations, levels of NPC1 protein, and phenotypes emphasize the functional significance of the putative sterol-sensing domain and of the cysteine-rich luminal loop. Am J Hum Genet 68: 1373-1385. https://doi.org/10.1086/320606.

Munkacsi, A. B., et al. (2011) An "exacerbate-reverse" strategy in yeast identifies histone deacetylase inhibition as a correction for cholesterol and sphingolipid transport defects in human Niemann-Pick type C disease. J Biol Chem 286: 23842-23851. https://doi.org/10.1074/jbc.M111.227645.

Musalkova, D., et al. (2020) Transcript, protein, metabolite and cellular studies in skin fibroblasts demonstrate variable pathogenic impacts of NPC1 mutations. Orphanet J Rare Dis 15: https://doi.org/10.1186/s13023-020-01360-5.

Nakasone, N., et al. (2014) Endoplasmic reticulum-associated degradation of Niemann-Pick C1: evidence for the role of heat shock proteins and identification of lysine residues that accept ubiquitin. J Biol Chem 289: 19714-19725. https://doi.org/10.1074/jbc.M114.549915.

Naureckiene, S., et al. (2000) Identification of HE1 as the Second Gene of Niemann-Pick C Disease. Science 290: 2298-2301. https://doi.org/10.1126/science.290.5500.2298.

Neufeld, E. B., et al. (1999) The Niemann-Pick C1 protein resides in a vesicular compartment linked to retrograde transport of multiple lysosomal cargo. J Biol Chem 274: 9627-9635. https://doi.org/10.1074/jbc.274.14.9627.

Newton, J., et al. (2017) FTY720/fingolimod increases NPC1 and NPC2 expression and reduces cholesterol and sphingolipid accumulation in Niemann-Pick type C mutant fibroblasts. FASEB J 31: 1719-1730. https://doi.org/10.1096/fj.201601041R.

Nietupski, J. B., et al. (2012) Iminosugar-based inhibitors of glucosylceramide synthase prolong survival but paradoxically increase brain glucosylceramide levels in Niemann-Pick C mice. Mol Genet Metab 105: 621-628. https://doi.org/10.1016/j.ymgme.2012.01.020.

Nunes, M. J., et al. (2013) Histone deacetylase inhibition decreases cholesterol levels in neuronal cells by modulating key genes in cholesterol synthesis, uptake and efflux. PLOS ONE 8: e53394. https://doi.org/10.1371/journal.pone.0053394.

Ohgane, K., et al. (2013) Discovery of oxysterol-derived pharmacological chaperones for NPC1: implication for the existence of second sterol-binding site. Chem Biol 20: 391-402. https://doi.org/10.1016/j.chembiol.2013.02.009.

Pacheco, C. D., et al. (2007) Autophagy in Niemann-Pick C disease is dependent upon Beclin-1 and responsive to lipid trafficking defects. Hum Mol Genet 16: 1495-1503. https://doi.org/10.1093/hmg/ddm100.

Pallottini, V., Pfrieger, F. W. (2020) Understanding and Treating Niemann-Pick Type C Disease: Models Matter. Int J Mol Sci 21: https://doi.org/10.3390/ijms21238979.

Patterson, M., Niemann-Pick Disease Type C. In: M. P. Adam, et al., (Eds.), GeneReviews(®). University of Washington, Seattle

Copyright © 1993-2022, University of Washington, Seattle. GeneReviews is a registered trademark of the University of Washington, Seattle. All rights reserved., Seattle (WA), 2020.

Patterson, M. C., et al. (2020) Long-term survival outcomes of patients with Niemann-Pick disease type C receiving miglustat treatment: A large retrospective observational study. J Inherit Metab Dis 43: 1060-1069. https://doi.org/10.1002/jimd.12245.

Patterson, M. C., et al. (2007) Miglustat for treatment of Niemann-Pick C disease: a randomised controlled study. Lancet Neurol 6: 765-772. https://doi.org/10.1016/S1474-4422(07)70194-1.

Pentchev, P. G., et al. (1985) A defect in cholesterol esterification in Niemann-Pick disease (type C) patients. Proc Natl Acad Sci USA 82: 8247-8251. https://doi.org/10.1073/pnas.82.23.8247.

Pfrieger, F. W. (2023) The Niemann-Pick type diseases - A synopsis of inborn errors in sphingolipid and cholesterol metabolism. Prog Lipid Res 90: 101225. https://doi.org/10.1016/j.plipres.2023.101225.

Pineda, M., et al. (2019) Disease characteristics, prognosis and miglustat treatment effects on disease progression in patients with Niemann-Pick disease Type C: an international, multicenter, retrospective chart review. Orphanet J Rare Dis 14: 32. https://doi.org/10.1186/s13023-019-0996-6.

Pineda, M., et al. (2018) Miglustat in Niemann-Pick disease type C patients: a review. Orphanet J Rare Dis 13: 140. https://doi.org/10.1186/s13023-018-0844-0.

Pipalia, N. H., et al. (2011) Histone deacetylase inhibitor treatment dramatically reduces cholesterol accumulation in Niemann-Pick type C1 mutant human fibroblasts. Proc Natl Acad Sci USA 108: 5620-5625. https://doi.org/10.1073/pnas.1014890108.

Pipalia, N. H., et al. (2021) HSP90 inhibitors reduce cholesterol storage in Niemann-Pick type C1 mutant fibroblasts. J Lipid Res 62: https://doi.org/10.1016/j.jlr.2021.100114.

Pipalia, N. H., et al. (2017) Histone deacetylase inhibitors correct the cholesterol storage defect in most Niemann-Pick C1 mutant cells. J Lipid Res 58: 695-708. https://doi.org/10.1194/jlr.M072140.

Platt, F. M., et al. (1994) N-butyldeoxynojirimycin is a novel inhibitor of glycolipid biosynthesis. J Biol Chem 269: 8362-8365.

Praggastis, M., et al. (2015) A murine Niemann-Pick C1 I1061T knock-in model recapitulates the pathological features of the most prevalent human disease allele. J Neurosci 35: 8091-8106. https://doi.org/10.1523/jneurosci.4173-14.2015.

Pugach, E. K., et al. (2018) High-content screen for modifiers of Niemann-Pick type C disease in patient cells. Hum Mol Genet 27: 2101-2112. https://doi.org/10.1093/hmg/ddy117.

Qian, H., et al. (2020) Structural Basis of Low-pH-Dependent Lysosomal Cholesterol Egress by NPC1 and NPC2. Cell 182: 98-111.e118. https://doi.org/10.1016/j.cell.2020.05.020.

Rangel, D. M., et al. (2020) Beyond the Typical Syndrome: Understanding Non-motor Features in Niemann-Pick Type C Disease. Cerebellum 19: 722-738. https://doi.org/10.1007/s12311-020-01156-0.

Rodriguez-Gil, J. L., et al. (2013) A somatic cell defect is associated with the onset of neurological symptoms in a lysosomal storage disease. Mol Genet Metab 110: 188-190. https://doi.org/https://doi.org/10.1016/j.ymgme.2013.06.010.

Sakamaki, J. I., et al. (2017) Bromodomain Protein BRD4 Is a Transcriptional Repressor of Autophagy and Lysosomal Function. Molecular Cell 66: 517-532. https://doi.org/10.1016/j.molcel.2017.04.027.

Schultz, M. L., et al. (2019) Synthetic high-density lipoprotein nanoparticles for the treatment of Niemann-Pick diseases. BMC Med 17: 200. https://doi.org/10.1186/s12916-019-1423-5.

Schultz, M. L., et al. (2018) Coordinate regulation of mutant NPC1 degradation by selective ER autophagy and MARCH6-dependent ERAD. Nat Commun 9: 3671. https://doi.org/10.1038/s41467-018-06115-2.

Schultz, M. L., et al. (2022) Species-specific differences in NPC1 protein trafficking govern therapeutic response in Niemann-Pick type C disease. JCI Insight 7: :e160308. https://doi.org/10.1172/jci.insight.160308.

Segatto, M., et al. (2017) Epigenetic targeting of bromodomain protein BRD4 counteracts cancer cachexia and prolongs survival. Nat Commun 8: 1707. https://doi.org/10.1038/s41467-017-01645-7.

Segatto, M., et al. (2020) BETs inhibition attenuates oxidative stress and preserves muscle integrity in Duchenne muscular dystrophy. Nat Commun 11: 6108. https://doi.org/10.1038/s41467-020-19839-x.

Shen, D., et al. (2012) Lipid storage disorders block lysosomal trafficking by inhibiting a TRP channel and lysosomal calcium release. Nat Commun 3: 731. https://doi.org/10.1038/ncomms1735.

Shen, H., et al. (2021) BRD2 regulation of sigma-2 receptor upon cholesterol deprivation. Life Sci Alliance 4: e201900540. https://doi.org/10.26508/lsa.201900540.

Shen, S. J., et al. (2020) BRD4 Inhibition Protects Against Acute Pancreatitis Through Restoring Impaired Autophagic Flux. Front Pharmacol 11: https://doi.org/10.3389/fphar.2020.00618.

Shorstova, T., et al. (2021) Achieving clinical success with BET inhibitors as anti-cancer agents. Br J Cancer 124: 1478-1490. https://doi.org/10.1038/s41416-021-01321-0.

Sitarska, D., et al. (2021) Treatment trials in Niemann-Pick type C disease. Metab Brain Dis 36: 2215-2221. https://doi.org/10.1007/s11011-021-00842-0.

Sleat, D. E., et al. (2004) Genetic evidence for nonredundant functional cooperativity between NPC1 and NPC2 in lipid transport. Proc Natl Acad Sci USA 101: 5886-5891. https://doi.org/10.1073/pnas.0308456101.

Solomon, B. I., et al. (2022) Phenotypic expression of swallowing function in Niemann-Pick disease type C1. Orphanet J Rare Dis 17: https://doi.org/10.1186/s13023-022-02472-w.

Stein, V. M., et al. (2012) Miglustat improves purkinje cell survival and alters microglial phenotype in feline niemann-pick disease type C. J Neuropathol Exp Neurol 71: 434-448. https://doi.org/10.1097/NEN.0b013e31825414a6.

Sugimoto, Y., et al. (2001) Accumulation of cholera toxin and GM1 ganglioside in the early endosome of Niemann-Pick C1-deficient cells. Proc Natl Acad Sci USA 98: 12391-12396. https://doi.org/10.1073/pnas.221181998.

Sui, S. Y., et al. (2019) Ferritinophagy is required for the induction of ferroptosis by the bromodomain protein BRD4 inhibitor (+)-JQ1 in cancer cells. Cell Death Dis 10: https://doi.org/10.1038/s41419-019-1564-7.

Taniguchi, M., et al. (2001) Sites and temporal changes of gangliosides GM1/GM2 storage in the Niemann-Pick disease type C mouse brain. Brain Dev. 23: 414-421. https://doi.org/10.1016/s0387-7604(01)00252-2.

te Vruchte, D., et al. (2004) Accumulation of glycosphingolipids in Niemann-Pick C disease disrupts endosomal transport. J Biol Chem 279: 26167-26175. https://doi.org/10.1074/jbc.M311591200.

te Vruchte, D., et al. (2014) Relative acidic compartment volume as a lysosomal storage disorder-associated biomarker. J Clin Invest 124: 1320-1328. https://doi.org/10.1172/jci72835.

Tonini, C., et al. (2020) Inhibition of Bromodomain and Extraterminal Domain (BET) Proteins by JQ1 Unravels a Novel Epigenetic Modulation to Control Lipid Homeostasis. Int J Mol Sci 21: 1297. https://doi.org/10.3390/ijms21041297.

Torres, S., et al. (2017) Mitochondrial GSH replenishment as a potential therapeutic approach for Niemann Pick type C disease. Redox Biol 11: 60-72. https://doi.org/10.1016/j.redox.2016.11.010.

Vacca, F., et al. (2019) Cyclodextrin triggers MCOLN1-dependent endo-lysosome secretion in Niemann-Pick type C cells. J Lipid Res 60: 832-843. https://doi.org/10.1194/jlr.M089979.

Vanier, M. T. (2010) Niemann-Pick disease type C. Orphanet J Rare Dis 5: 16. https://doi.org/10.1186/1750-1172-5-16.

Vanier, M. T., et al. (1991) Type C Niemann-Pick disease: spectrum of phenotypic variation in disruption of intracellular LDL-derived cholesterol processing. Biochim Biophys Acta 1096: 328-337. https://doi.org/10.1016/0925-4439(91)90069-l.

Vichaikul, S., et al. (2022) Inhibition of bromodomain extraterminal histone readers alleviates skin fibrosis in experimental models of scleroderma. JCI Insight 7: https://doi.org/10.1172/jci.insight.150871.

Völkner, C., et al. (2022) Assessment of FDA-Approved Drugs as a Therapeutic Approach for Niemann-Pick Disease Type C1 Using Patient-Specific iPSC-Based Model Systems. Cells 11: 319. https://doi.org/10.3390/cells11030319.

Wakita, M., et al. (2020) A BET family protein degrader provokes senolysis by targeting NHEJ and autophagy in senescent cells. Nat Commun 11: 1935. https://doi.org/10.1038/s41467-020-15719-6.

Wang, C., et al. (2019) Quantitating the epigenetic transformation contributing to cholesterol homeostasis using Gaussian process. Nat Commun 10: 5052. https://doi.org/10.1038/s41467-019-12969-x.

Wang, C., et al. (2020) Individualized management of genetic diversity in Niemann-Pick C1 through modulation of the Hsp70 chaperone system. Hum Mol Genet 29: 1-19. https://doi.org/10.1093/hmg/ddz215.

Wang, H., et al. (2016) Ebola Viral Glycoprotein Bound to Its Endosomal Receptor Niemann-Pick C1. Cell 164: 258-268. https://doi.org/10.1016/j.cell.2015.12.044.

Wassif, C. A., et al. (2016) High incidence of unrecognized visceral/neurological late-onset Niemann-Pick disease, type C1, predicted by analysis of massively parallel sequencing data sets. Genet Med 18: 41-48. https://doi.org/10.1038/gim.2015.25.

Wehrmann, Z. T., et al. (2012) Quantitative comparison of the efficacy of various compounds in lowering intracellular cholesterol levels in Niemann-Pick type C fibroblasts. PLOS ONE 7: e48561. https://doi.org/10.1371/journal.pone.0048561.

Winkler, M. B. L., et al. (2019) Structural Insight into Eukaryotic Sterol Transport through Niemann-Pick Type C Proteins. Cell 179: 485-497.e418. https://doi.org/10.1016/j.cell.2019.08.038.

Xu, M., et al. (2012) δ-Tocopherol reduces lipid accumulation in Niemann-Pick type C1 and Wolman cholesterol storage disorders. J Biol Chem 287: 39349-39360. https://doi.org/10.1074/jbc.M112.357707.

Xu, M., et al. (2014) A Phenotypic Compound Screening Assay for Lysosomal Storage Diseases. J Biomol Screen 19: 168-175. https://doi.org/10.1177/1087057113501197.

Yamamoto, T., et al. (2000) Genotype-phenotype relationship of Niemann-Pick disease type C: a possible correlation between clinical onset and levels of NPC1 protein in isolated skin fibroblasts. J Med Genet 37: 707-712. https://doi.org/10.1136/jmg.37.9.707.

Yambire, K. F., et al. (2019) Mitochondrial biogenesis is transcriptionally repressed in lysosomal lipid storage diseases. Elife 8: https://doi.org/10.7554/eLife.39598.

Yilmaz, S. B., et al. (2020) Clinical and Molecular Features of Early Infantile Niemann Pick Type C Disease. Int J Mol Sci 21: https://doi.org/10.3390/ijms21145059.

Yu, T., et al. (2012) Ryanodine receptor antagonists adapt NPC1 proteostasis to ameliorate lipid storage in Niemann-Pick type C disease fibroblasts. Hum Mol Genet 21: 3205-3214. https://doi.org/https://doi.org/10.1093/hmg/dds145.

Yu, W., et al. (2005) Altered cholesterol metabolism in Niemann-Pick type C1 mouse brains affects mitochondrial function. J Biol Chem 280: 11731-11739. https://doi.org/10.1074/jbc.M412898200.

Zampieri, S., et al. (2012) Treatment of Human Fibroblasts Carrying NPC1 Missense Mutations with MG132 Leads to an Improvement of Intracellular Cholesterol Trafficking. JIMD Rep 2: 59-69. https://doi.org/10.1007/8904_2011_49.

Zervas, M., et al. (2001a) Neurons in Niemann-Pick disease type C accumulate gangliosides as well as unesterified cholesterol and undergo dendritic and axonal alterations. J Neuropathol Exp Neurol 60: 49-64. https://doi.org/10.1093/jnen/60.1.49.

Zervas, M., et al. (2001b) Critical role for glycosphingolipids in Niemann-Pick disease type C. Curr Biol 11: 1283-1287. https://doi.org/10.1016/s0960-9822(01)00396-7.

Zhang, M., et al. (2001) Cessation of rapid late endosomal tubulovesicular trafficking in Niemann-Pick type C1 disease. Proc Natl Acad Sci USA 98: 4466-4471. https://doi.org/10.1073/pnas.081070898.

Zhang, M., et al. (2003) Differential trafficking of the Niemann-Pick C1 and 2 proteins highlights distinct roles in late endocytic lipid trafficking. Acta Paediatrica 92: 63-73. https://doi.org/10.1080/08035320310021958.

Zou, M., et al. (2022) Inhibition of cGAS-STING by JQ1 alleviates oxidative stress-induced retina inflammation and degeneration. Cell Death Differ 29: 1816-1833. https://doi.org/10.1038/s41418-022-00967-4.